Design of a SF_6-Gas-Filled Spark Gap Switch for High-Voltage Application

H. Rahaman, H. Heo, S. S. Park, and Sang H. Nam, *Member, IEEE*

***Abstract*—It is our endeavor to develop switching technology for the breakdown reliability and reproducibility at extremely high voltages above 1 MV. One of the key objectives of the endeavor is to derive precise breakdown criteria for use in high-voltage applications. We have developed empirical criteria by which the breakdown field strength of a high-pressure SF_6-filled spark gap can be computed. The validity of the computed result has been verified with several experimental data from different investigators. The computed result has shown good agreement in an extended range of pd (pressure times gap distance) and field enhancement factor of the spark gap geometry. Furthermore, a spark gap has been designed and constructed with particular intention of generating a high-pulsed-power source in Pohang Accelerator Laboratory. In parallel, field modeling has been performed to verify the appropriate shape of the highly stressed insulator and electrode design in the spark gap and to evaluate their field enhancements. A series of breakdown voltage tests has demonstrated the function of the spark gap switch as intended up to 9 bars of SF_6. Aside from this, the limitation of the switching behavior has been examined with an aim of operating the designed spark gap to its maximum capability.**

***Index Terms*—Breakdown strength, field enhancement, high-pressure SF_6 gas, spark gap switch.**

I. Introduction

THE DESIGN and construction of the SF_6-gas-filled spark gap, as well as its operation, are extensively investigated in various applications like in circuit breakers, gas-insulated substations, and laboratory works, viz., in Marx generators, pulse-forming networks, and other high-energy pulsed-power systems for applications requiring very high voltages and extremely high currents [1]–[4]. It is indeed difficult to predict the electrical breakdown strength of the high-pressure SF_6-filled spark gap with the available reference data. The reported data in literatures are not always measured under the same test parameters, and in many cases, the test conditions are not fully described. The experimental data, as well as few empirical formulas, from which the breakdown field strength can be calculated are valid with certain voltage and field conditions or pressure ranges. Therefore, their extrapolation to very high voltages leads to an error. Even though the breakdown field strength at high voltages exceeding 1 MV in a nonuniform field gap has many applications in pulsed power, there exists very limited information that can be used for the design of the SF_6-filled spark gap at these voltages.

The empirical criteria to compute the breakdown field strength of high-pressure SF_6 gas in a nonuniform spark gap have been newly established by Nam *et al.* which are modified work of J. C. Martin and E. Kuffel *et al.* [1], [2], [5], [6]. The criteria for the breakdown field strength are provided by J. C. Martin for the nonuniform electrode gap in air and by E. Kuffel *et al.* for the uniform electrode gap in SF_6 gas. The aforementioned criteria are exploited for the design of the spark gap switch to function as intended in our laboratory application. The comparison, between data of different investigators and our empirical criteria, shows a very satisfactory degree of agreement. For practical importance, we have focused on the influence of the field enhancement, neglecting the temporal development of voltage stress across the electrode shapes being used. Furthermore, to confirm the accuracy of the criteria, a spark gap has been designed and constructed in-house. The breakdown voltage of the spark gap against the SF_6 gas pressure up to 9 bars has been measured. The limiting behavior of the gas pressure and applied voltage values has also been observed. The breakdown voltage measurement above 9 bars led to the switch failure. The failure has been analyzed to scale the operation of the designed spark gap switch to its maximum voltage and pressure handling capability.

II. Theory

High-pressure spark gaps possess many characteristics which are suited to pulsed-power applications such as wide voltage and current handling capability (up to levels of megavolts and megaamperes), nanosecond closing time, low jitter, charging ability of several times higher than the dc breakdown voltage, and simplicity in the design. The switch closing process starts with the application of the voltage across the gap beyond a certain threshold voltage. This initiates an electron avalanche in the gap which grows to a point where the space charge field establishes a highly conducting plasma channel so-called a streamer [2], [3], [7], [8]. The streamer propagates across the gap to develop a conducting channel. The voltage drops essentially to zero compared to the hold-off voltage, and the switch is considered to be closed. Based on the aforementioned theory, we have established the field strength of the SF_6 gas in the nonuniform electrode gap as follows [5], [6].

Manuscript received September 30, 2009; revised December 17, 2009 and March 5, 2010; accepted May 5, 2010. Date of publication June 28, 2010; date of current version October 8, 2010.

The authors are with Pohang Accelerator Laboratory, Pohang University of Science and Technology, Pohang 790-784, Korea (e-mail: hasib@postech.ac.kr; heohoon@postech.ac.kr; sspark@postech.ac.kr; nsh@postech.ac.kr).

Color versions of one or more of the figures in this paper are available online at http://ieeexplore.ieee.org.

Digital Object Identifier 10.1109/TPS.2010.2052361

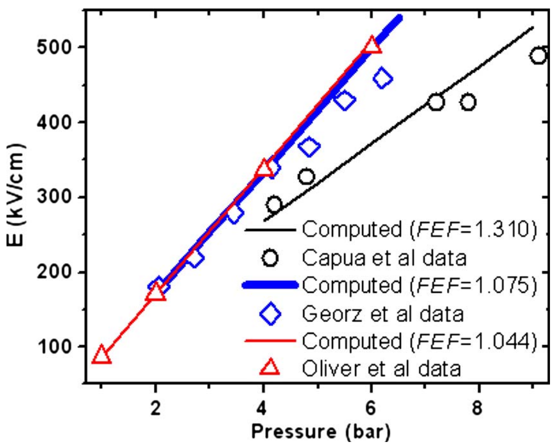

Fig. 1. Comparison of mean electric field from different investigators.

At low pressure $(pd \leq 3\ \text{bar} \cdot \text{cm})$

$$E_{\max} = 88.5p + 0.65\beta/d_{\text{eff}}\ [\text{kV/cm}]. \tag{1}$$

At high pressure $(pd > 3\ \text{bar} \cdot \text{cm})$

$$E_{\max} = 68p + 40\beta/d_{\text{eff}}\ [\text{kV/cm}] \tag{2}$$

where $E_{\max}$ is the maximum electric field that takes into account the field enhancement factor (FEF) of the spark gap electrode geometry. $E_{\max}$ is related with the mean field E through the relation

$$FEF = E_{\max}/(V/d) = E_{\max}/E. \tag{3}$$

To calculate the maximum breakdown field, J. C. Martin considered the characteristic distance of the field falloff where the electron avalanche leads to the start of the streamer [1]. This field falloff length is a function of the geometry and corresponds to an effective distance d_{eff}. For example, $d_{\text{eff}} = 0.115r$ for spheres, and $d_{\text{eff}} = 0.23r$ for cylinders, where r is the radius. If the gap length is below d_{eff}, then the ionization diminishes out, and subsequently, no breakdown occurs. β in (1) and (2) is a correction curve that includes the effect of the FEF and is generalized as [5], [6]

$$\beta = 0.987 - 1.805 \times \sqrt{0.582/x} \times I_1(13.871 \times \sqrt{x})/\left(\exp\left(5.291 + (x/0.110)\right)\right) \tag{4}$$

where I_1 is the modified Bessel function of the first kind, I_α is of order 1 $(\alpha = 1)$, and x is the variable d/r.

To validate our criteria [(1) and (2)] of breakdown in SF_6 gas, the data from different investigators are collected and compared, as shown in Fig. 1. Here, the computed result and measured data have been plotted for the mean field E. The measured data by Di Capua *et al.* (marked by circles), Goerz *et al.* (marked by rectangles), and Olivier *et al.* (marked by triangles) in the pd range of 14.2–35.5 bar · cm, 0.5–1.75 bar · cm, and 1–6 bar · cm, respectively, have a very good agreement with our breakdown field strength criteria [5], [6], [9]–[11]. These three cases highlight the fact that our computed criteria agree not only for an extended range of pd but also for a wide range of FEF. It is to be noted that the temporal effect of voltage pulses in all the aforementioned cases is ignored.

Fig. 2. Prototype spark gap switch.

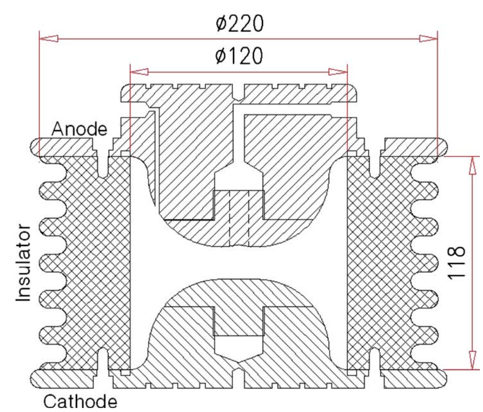

Fig. 3. Cross-sectional view of the spark gap switch.

III. Design and Construction

Fig. 2 shows the prototype spark gap switch. In this particular design, r and β are 4 cm and 0.794, respectively, with the FEF of 1.1025. The cross-sectional view of the spark gap is shown in Fig. 3 with assembled major components. The spark gap switch is assembled in a cylindrical housing, which is an insulator, with the main metal electrodes at the top and bottom of it. Each of the metal electrodes of stainless steel (SS) has a spherical edge to minimize the FEF. These electrodes are fixed at each end of the cylindrical insulator by eight metallic bolts (SUS M6). The corresponding threads are SS metallic spring of 14-mm depth inside the insulator. The insulator envelope is made of monocast nylon (MC 901) type, which is blue in color [12]. The insulator is chosen for its low dielectric constant which reduces the electrical stress along its surface [13]. Furthermore, the insulation is improved due to its corrugated structure at the outside envelope. The corrugated structure of the insulator increases the creepage length between the electrodes. Aside from these facts, the monocast nylon offers superior mechanical strength and durability among the most commercial type nylon

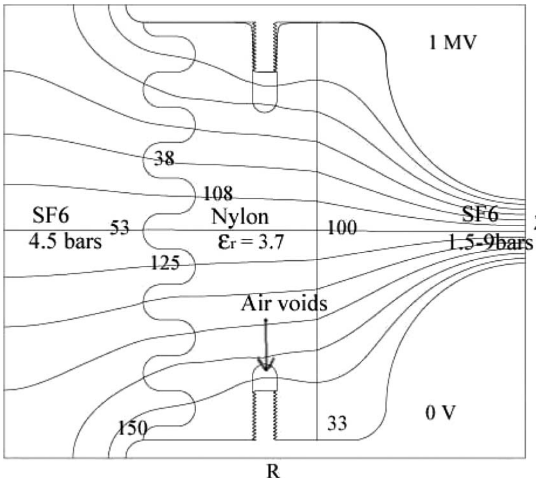

Fig. 4. Field modeling results. The contours are equipotential lines, and the illustrated values are electric field strengths in kilovolts per centimeter.

grades, as well as high thermal stability up to 127 °C. The inner and outer radii of the nylon insulator are 6 and 11.0 cm, respectively. The closest distance between the main electrodes is 1.8 cm, while along the insulator, the distance increases to 11.8 cm. Thus, the distance between the electrodes from the center axis to the outward is sized according to a desired operating level of voltage and SF_6 pressure. In addition, two holes are drilled through the anode electrode to control the pressure inside the spark gap switch. The yield strength of the envelope material has no problem holding pressures above 10 bars. However, the pressure is limited to 10 bars due to the connecting tube between the spark gap and the SF_6 bottle.

Fig. 4 shows the field modeling results with contours of equipotential lines. The numbers shown are electric field values in kilovolts per centimeter. A Field Precision program has been used for the developed design to provide information about potential and electric fields [14]. Our requirement is to generate rectangular voltage pulses at the load exceeding 500 kV with a pulsewidth of above 200 ns [15]. From a single transmission line theory, it is a known fact that the voltage across the output load is one-half of the applied voltage across the switch if the load impedance is matched with the source impedance [8], [16]. Therefore, the applied voltage, to start the breakdown in SF_6, at the anode is 1 MV in the designed model. Although the modeling does not provide temporal effect of the applied voltage, it allows correcting our empirical criteria for the SF_6 breakdown strength by including the effect of the field enhancement of different shaped assemblies. Furthermore, we can identify the limiting features of the designed spark gap operation such as maximum voltage and pressure values. The relative dielectric constant of the nylon insulator is 3.7 [12]. The nylon spacer with metal inserts at each end produces different electric field strengths. The triple points (metal–insulator–gas) inside the spark gap envelope have a very low electrical stress of 33 kV/cm. The maximum field stress, along the inside region of the envelope insulator–gas interface, is almost in the middle way, which is about 100 kV/cm. The strongest field stress along the outside region of the envelope insulator–gas interface is in the halfway, which is about 125 kV/cm. The triple points outside the spark gap envelope have an electrical stress of 150 kV/cm. All these stress values are below the threshold breakdown strength of the insulator, as well as the SF_6 gas. The threshold breakdown strength of the monocast nylon insulator is 200 kV/cm, while for the SF_6 gas, it will vary with pressures. Thus, the design shapes of the metal electrodes and insulator surfaces have been properly managed for the electric stress to guarantee the breakdown of the spark gap above 1 MV.

TABLE I
PFN-MARX DESIGN SPECIFICATION

Parameter	Value
Total number of PFN stage	33
Total number of PFN sections in each stage	4
PFN capacitance each stage	32 nF
PFN inductance each stage	400 nH
Pulse width	226 ns
Rise time	10's of ns
PFN impedance each stage	3.54 Ω
Total PFN-Marx impedance	117 Ω

IV. TEST SETUP AND PROCEDURE

A setup facility for testing the high-voltage spark gap switch has been developed in-house at Pohang Accelerator Laboratory. The purpose of this experiment is to establish a bearing parameter setting on the pressure of the SF_6 gas, on the gap spacing, and on the geometry effect (or the FEF) by which the breakdown criteria can be calculated with more precisely. A 33-stage PFN-Marx system is designed and fabricated for generation of high-voltage test pulses [15]. The typical design parameters of the PFN-Marx system are given in Table I. In application, we have established that a water load of about 150-Ω impedance is matched with the PFN-Marx system [5], [6]. The increase of the impedance than the designed value could be due to the stray inductance in the PFN sections per stage. The PFN-Marx tank is filled with 4.5 bars of SF_6 in order to prevent breakdown inside the Marx tank wall as well as increase the flashover voltage along the outer housing insulator of the spark gap.

The Marx system is charged by a power supply through a current-limiting resistor of 50 kΩ. Then, the voltage of the power supply is increased in a following manner. The voltage is increased in a step of 0.1 kV until the self-breakdown voltage of the tested spark gap at a given pressure is attained. The increment of the supply voltage up to three to four steps is continued to ensure the self-breakdown regime. Then, the supply voltage is again decreased in similar steps to ensure the threshold level of the self-breakdown regime below which no more breakdown is possible. Such measurement data are noted for different SF_6 pressures of the spark gap in a step of 1 bar except the first one which has the pressure increment of 0.5 bar. We have tested the performance of the constructed switch over the desired range of operating parameters.

V. TEST RESULT AND DISCUSSION

The output waveform is determined not only by the PFN elements of the Marx system but also by firing characteristics

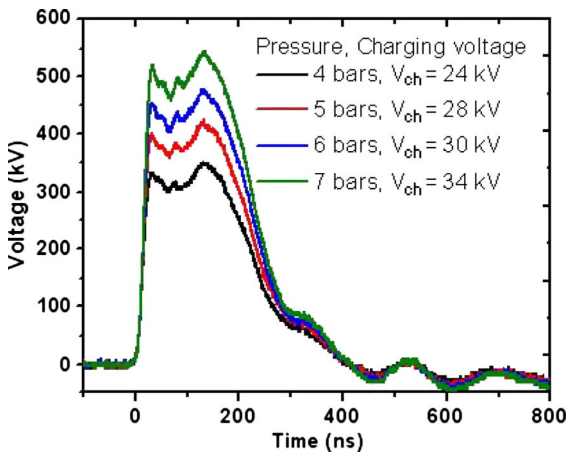

Fig. 5. Temporal behavior of output voltage waveforms at different pressures.

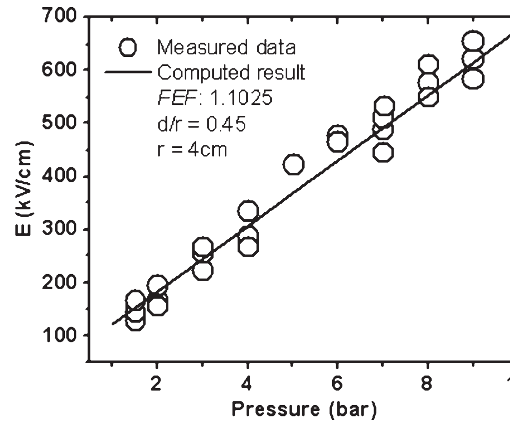

Fig. 6. Comparison of mean electric field between experimental data and computed result. Circles are the measured data.

of the switch itself and the circuit elements (capacitance and inductance) between the spark gap and the load. The high-pressure SF_6-filled spark gap switch, which can be said to be the peaking gap, is coupled at the end of the Marx system to generate a fast-rise-time pulse waveform at the load. The temporal behavior of some typical output voltage waveforms is shown in Fig. 5. The corresponding charging voltages from the power supply, as well as the pressures, are also illustrated. The voltage waveforms have the 10%–90% rise time of less than 25 ns, while the pulsewidth at a full width at half maximum is about 230 ns.

The main components that decide the rise time of the output voltage pulses are stray values of capacitance and inductance, as well as the load impedance. Resistive and inductive phase times of the spark gap, which also take, in part, a role to decide the switching rise time, are a function of the gas density and the spark gap geometry, respectively [1], [3]. In order to minimize the intrinsic inductance and, thus, the pulse rise time, the gap spacing and the spark gap geometry are chosen as small as possible. The combined effect of the resistive and inductive phase times of the spark gap is very small (< 2 ns). In addition, the stray capacitance formed around the spark gap, which works as a peaking gap capacitance, has very small effect on the rise time (< 1 ns) of the output voltage waveforms. Therefore, the rise time of few tens of nanoseconds is mainly due to the circuit stray inductance formed between the spark gap and the load.

Fig. 6 shows the experimental data points and the computed mean electric field strength of the designed spark gap switch as a function of the absolute SF_6 pressure. The pd value has a range of 2.7–16.2 bar · cm. The empty circles represent the measured self-breakdown field strength. The computed breakdown field strength shown by the solid line is in good agreement with the measured data. The spark gap operated very well up to 9 bars of SF_6, which corresponds to about 1.1 MV of the breakdown voltage. Further experiments above 9 bars led to the switch failure. After carrying out switching action for two to three times at 10 bars, the pressure of the spark gap dropped quickly to the tank pressure, which indicated broken pressure sealing of the spark gap housing.

After the failure, the spark gap switch was dissembled for inspection. Close photographs of the dissembled insulator are

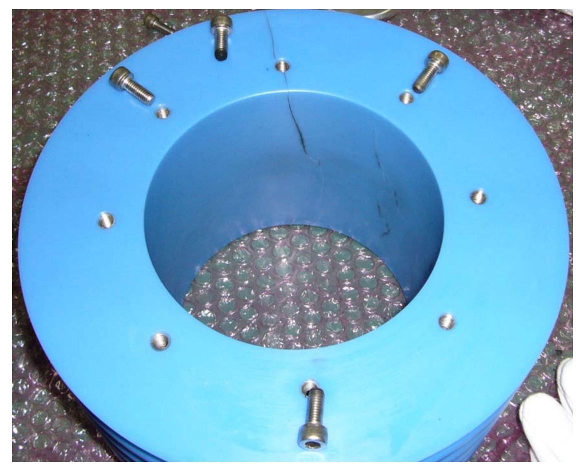

Fig. 7. Insulator cracks starting from the thread holes and stretched along the inside wall. The bottom tips of the screws are burned due to discharges.

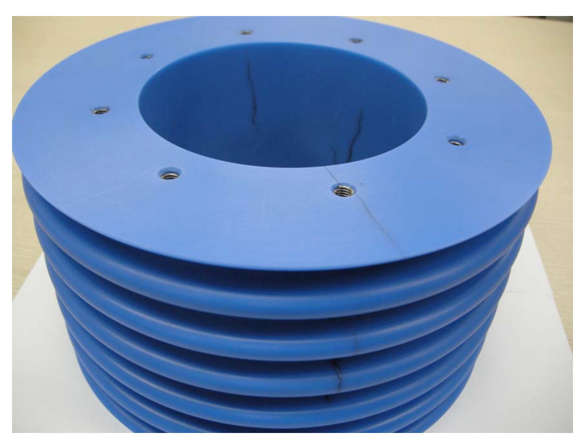

Fig. 8. Cracks are stretched along the outside wall of the corrugated spacer.

shown in Figs. 7 and 8. At the pressure of 10 bars, the expected breakdown voltage of the spark gap is greater than 1.2 MV. Therefore, a very high voltage stress (above 200 kV/cm) exists at the triple points near the screws which are used for mechanical support. Moreover, trapped atmospheric air in voids enhances the breakdown. The size of air voids was about

5–10 mm in length and 6 mm in diameter. Failures might be ascribed by the highly electrical stress at the triple junctions of the voids. In fact, these triple junctions, in general, constitute the weakest electrical location. The local field enhancement at these junctions influences the discharge development in the air voids. The discharge then occurred through the insulator and eventually led to the insulator crazes to breakdown the spark gap. The crazing became worse with few shots of charging the Marx system above 1.2 MV after which the pressure of the spark gap deteriorated strongly.

During inspection, we have found cracks on the inside wall of the insulator. The cracks have connected two opposite thread holes. Many screws have shown burning bottom edges which imply the occurrence of discharges in the voids. One of the cracks extended to the top of the insulator surface, even to the outside insulator surface. The appearance of the cracks in the insulator material was the reason that led to the pressure failure of the spark gap operation.

We consider several solutions to overcome the aforementioned failure. To avoid air void failures, we are planning to fill the voids with SF_6 by providing a small gas path in the screws and replace the metallic screws with insulator ones that have enough yield strength to hold the spark gap envelope with a SF_6 pressure of more than 10 bars. With such solutions, the SF_6-filled spark gap design might be extended to higher field strength or higher operating voltage.

VI. Conclusion

The newly developed criteria of the electrical breakdown strength in the high-pressure SF_6-filled spark gap switch have been described in this paper. The criteria, which take into account the FEF of the spark gap geometry, have high accuracy. The computed result from the criteria agrees very well with several published data points. To further confirm the criteria, a spark gap switch and a high-voltage Marx system have been designed and constructed in-house. The designed spark gap operated well as intended up to the pressure of 9 bars and more than 1 MV of the applied voltage. The stringent limitations of the maximum operating pressure and breakdown voltage are due to the mechanical construction of the present spark gap. The failure of the spark gap has been demonstrated and correctly predicted by the field modeling results. Future work is planned to improve the design of the spark gap switch to generate the most reliable and reproducible voltage pulses for a relatively large pulsed-power system and a higher repetition rate of about 10 Hz.

References

[1] T. H. Martin, A. H. Guenther, and M. Kristiansen, *J.C. Martin on Pulsed Power*. New York: Plenum, 1996, ser. Advances in Pulsed Power Technology Series.

[2] E. Kuffel and W. S. Zaengl, *High Voltage Engineering Fundamentals*. New York: Pergamon, 1984.

[3] M. Khalifa, *High Voltage Engineering*. New York: Marcel Dekker, 1990.

[4] G. Schaefer, M. Kritiansen, and A. Guenther, *Gas Discharge Closing Switches*. New York: Plenum, 1990.

[5] S. H. Nam, H. Rahaman, H. Heo, S. S. Park, J. W. Shin, J. H. So, and W. Jang, "Analytical prediction of high pressure SF6 gas breakdown in a spark gap switch," in *Proc. IEEE Int. Power Modulator High Voltage Conf.*, May 2008, pp. 37–40.

[6] S. H. Nam, H. Rahaman, H. Heo, S. S. Park, J. W. Shin, J. H. So, and W. Jang, "Empirical analysis of high pressure SF6 gas breakdown strength in a spark gap switch," *IEEE Trans. Dielectr. Elect. Insul.*, vol. 16, no. 4, pp. 1106–1110, Aug. 2009.

[7] A. Pederson, "Criteria for spark breakdown in sulphur hexafluoride," *IEEE Trans. Power App. Syst.*, vol. PAS-89, no. 8, pp. 2043–2048, Nov. 1970.

[8] P. W. Karlsson and A. Pedersen, "Inherent limitations in uniform field discharge data for SF_6," *IEEE Trans. Power App. Syst.*, vol. PAS-91, no. 4, pp. 1597–1601, Jul. 1972.

[9] M. S. Di Capua, E. K. Freytag, W. R. Dixon, and R. A. Hawley, "A simple self-breaking 2 MV gas switch," in *Proc. 6th IEEE Pulsed Power Conf.*, 1987, pp. 518–521.

[10] D. A. Goerz, M. J. Wilson, and R. D. Speer, "A low profile high voltage compact gas switch," in *Proc. 11th IEEE Pulsed Power Conf.*, 1997, pp. 328–333.

[11] G. Olivier, Y. Gervais, and D. Mukhedkar, "A new approach to compute uniform field breakdown of gases," *IEEE Trans. Power App. Syst.*, vol. 97, no. 3, pp. 969–976, May 1978.

[12] [Online]. Available: http://www.platech.com

[13] J. R. Laghari and A. H. Qureshi, "Surface flashover of spacers in compressed gas insulated systems," *IEEE Trans. Elect. Insul.*, vol. EI-16, no. 5, pp. 373–387, Oct. 1981.

[14] *Finite-Element Software for Electromagnetics*, Field Precision, Albuquerque, NM, 2000. [Online]. Available: http://www.fieldp.com

[15] S. S. Park, H. Heo, O. L. Choi, S. H. Kim, S. C. Kim, S. H. Kim, Y. J. Park, Y. W. Son, M. S. Hong, J. H. Shu, S. H. Nam, J. W. Shin, J. H. So, and W. Jang, "Repetitive test of PFN Marx for pulse generator," in *Proc. 28th IEEE Power Modulator Symp.*, Las Vegas, NV, May 28–31, 2008, unpublished.

[16] G. N. Glasoe and J. V. Lebacqz, *Pulse Generators*. New York: McGraw-Hill, 1948, ser. MIT Radiation Laboratory Series.

H. Rahaman was born in Durgapur, India, on July 10, 1974. He received the Ph.D. degree in plasma physics from the University of Erlangen Nuremberg, Erlangen, Germany, in 2007.

From 2001 to 2002, he was a Research Assistant with the Central Electronics Engineering Research Institute, Pilani, India. Since August 2007, he has been a Researcher with Pohang Accelerator Laboratory, Pohang University of Science and Technology, Pohang, Korea. His current research includes the development of megavolt spark gap switches, very high repetitive spark gap switches, and pseudospark switches.

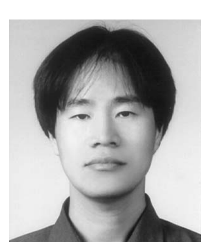

H. Heo was born in Seoul, Korea, on January 27, 1969. He received the Ph.D. degree from Kyungpook National University, Daegu, Korea, in 2002.

Since 2002, he has been with Pohang Accelerator Laboratory, Pohang University of Science and Technology, Pohang, Korea. His research interests include the development of Marx generators, high-voltage spark gap switches, TVS, and pseudospark switches.

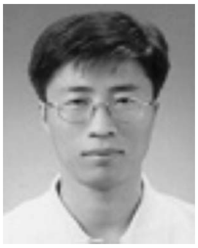

S. S. Park was born in Seoul, Korea, on February 15, 1965. He received the M.S. degree in electrical engineering from Chungbuk National University, Cheongju, Korea, in 1991.

Since 1991, he has been a Research Assistant with Pohang Accelerator Laboratory, Pohang University of Science and Technology, Pohang, Korea. His working areas are pulsed-power technology and high current switching. His research interests include the development of high-power switches based on the TVS, the pseudospark discharge, the high-voltage Marx generator for S-band klystrons, and the high-voltage transformers for high frequency.

Sang H. Nam (S'88–M'89) received the Ph.D. degree in electrical engineering from the University of South Carolina, Columbia, in 1990.

Since 1991, he has been the Chief Researcher with Pohang Accelerator Laboratory (PAL), Pohang University of Science and Technology, Pohang, Korea, where he is also currently the Deputy Director of PAL. During the construction of Pohang Light Source that is a 2.5-GeV electron accelerator facility, he developed the 200-MW modulators for 80-MW klystrons, the kicker modulator, and the 60-kW 500-MHz CW RF amplifiers. His research interests are in the areas of pulsed-power technology, power electronics, and high-power plasma switches.